1 *Article*

2 # Development of a pattern recognition methodology
3 # with thermography and implementation in an
4 # experimental study of a boiler for a WHRS-ORC

5 **Concepción Paz [1,*], Eduardo Suárez [1], Miguel Concheiro [1] and Antonio Diaz [1]**

6 [1] School of Industrial Engineering, University of Vigo, Campus Universitario Lagoas-Marcosende, 36310,
7 Spain; suarez@uvigo.es (E.S.); mconcheiro@uvigo.es (M.C.); adiaz@uvigo.es (A.D.)
8 * Correspondence: cpaz@uvigo.es; Tel.: +34 986 813 754

9

10 **Abstract:** Waste heat dissipated in the exhaust system in a combustion engine represents a major
11 source of energy to be recovered and converted into useful work. A waste heat recovery system
12 (WHRS) based on an Organic Rankine Cycle (ORC) is a promising approach, and has gained interest
13 in the last few years in an automotive industry interested in reducing fuel consumption and exhaust
14 emissions. Understanding the thermodynamic response of the boiler employed in an ORC plays an
15 important role in steam cycle performance prediction and control system design. The aim of this
16 study is therefore to present a methodology to study these devices by means of pattern recognition
17 with infrared thermography. In addition, the experimental test bench and its operating conditions
18 are described. The methodology proposed identifies the wall coordinates, traces paths, and tracks
19 wall temperature along them in a way that can be exported for subsequent post-processing and
20 analysis. As for the results, through the wall temperature paths on both sides (exhaust gas and
21 working fluid) it was possible to quantitatively estimate the temperature evolution along the boiler
22 and, in particular, the beginning and end of evaporation.

23 **Keywords:** WHRS; ORC; boiler; infrared thermography.
24

25 ## 1. Introduction

26   Increasingly restrictive international regulations concerning greenhouse gas emissions demand
27 the development of cleaner and more efficient internal combustion engines (ICEs). Most modern
28 diesel engines are achieving a maximum of about 35% in thermal efficiency—the remaining heat is
29 simply wasted. Waste heat is dissipated through three main channels: the coolant system, convection
30 and radiation from the engine block, and—most importantly—the exhaust system, which alone
31 accounts for up to 40% of total fuel energy [1–4].
32   In the last few years, the automotive industry has shown great interest in waste heat recovery
33 systems (WHRS) based on an Organic Rankine Cycle (ORC) because of its potential for recovering
34 some of that energy. This would achieve significant reductions in fuel consumption and, as a result,
35 exhaust emissions [4–6]. This technology has already been widely implemented over the past decade
36 in the marine sector [7-8], but reducing the components of the cycle to the scale of a passenger vehicle
37 is still a challenge. Nevertheless, there is room to work with in heavy duty vehicles, and so work has
38 continued[9].
39   Predicting the behavior of a boiler is fundamental in the development and design process of
40 these systems. Most boiler load losses are due to the superheated steam zone, so it is very important
41 to estimate its length adequately. In principle, there are correlations that can be used to predict a
42 boiler's thermal efficiency and head loss. These correlations are different for each section, though, so
43 determining the location of phase changes in a boiler is essential.
44   This study sets out to do just that using a test bench with an ORC-WHRS boiler. We study it
45 from two different approaches: on one hand, the monitored sensors retrieve overall parameters of

the boiler, such as outlet temperature, pressure drop, and performance; on the other hand, an infrared (IR) thermographic camera captures thermal images of the external walls of the boiler.

IR thermography is a non-contact and non-destructive technique well consolidated and applied in a wide range of fields, such as medicine and the military [10]. There is even some existing research in the literature that studies multiphase heat transfer processes with thermographic analysis. Liu and Pan [11] developed a method to measure the fluid temperature in parallel with the visualization of the two-phase flow pattern in micro channels. Hetsroni et al. [12] use an IR technique to investigate a heat sink for electronics cooling at low heat fluxes and to maintain the temperature of the heated surface at uniform temperatures. Xu et al. [13] carried out boiling heat transfer experiments where an IR high-speed camera was used to measure a chip's surface temperature and identify transient flow patterns in an array of triangular silicon-based microchannels. Li and Hrnjak [14] presented an IR thermography-based method to quantify the distribution of liquid refrigerant mass flow rate in a parallel flow microchannel heat exchanger. Leblay et al. [15] measured heat transfer coefficients of water flowing in a round tube and in a multiport flat tube. Carlomagno et al. [16] analyzed the ability of IR thermography to perform convective heat transfer measurements and surface visualizations in complex fluid flows.

In the present study, IR thermography has been used to experimentally analyse single phase and multiphase flows involved in the boiler of an ORC. Although the working fluid (WF) is not optically accessible, thermography allows us to quantitatively estimate and understand the fluid dynamic behaviour development of both the gas and the working fluid by inferring their properties from the wall temperatures of their adjacent walls. This study is focused on the implementation of a methodology capable of systematically handling a big database of these thermal images, based on a pattern recognition scheme, which automatically detects the boiler and extracts the temperatures to be analysed.

The rest of this paper is divided in three sections. Section 2 describes the experimental setup and the boiler of study. Section 3 presents the methodology developed. Section 4 shows and discusses the results obtained, our conclusions, and an overview of future work.

2. Experimental setup

The experimental test bench has been conceived as a tool to test boilers for implementation in an ORC-based WHRS for the automotive industry. The working fluid must have a high critical temperature, as well as high condensation and evaporation temperatures, suitable for a high-temperature ORC system. Among the fluids that meet these requirements—such us ethanol, R1233zd, siloxane, or n-octane— ethanol was chosen because of its low environmental impact and low health risks [17]. Furthermore, when the facilities were designed, ethanol was the working fluid of choice for many automotive manufacturers.

The test bench has three circuits: air, ethanol, and water refrigerant. Ethanol is preheated and pumped to the evaporator, where it comes into contact with previously warmed air. After that, the ethanol is cooled in the condenser by transferring its heat to the refrigeration water. Figure 1 shows a scheme of the hydraulic circuit and its characteristics.
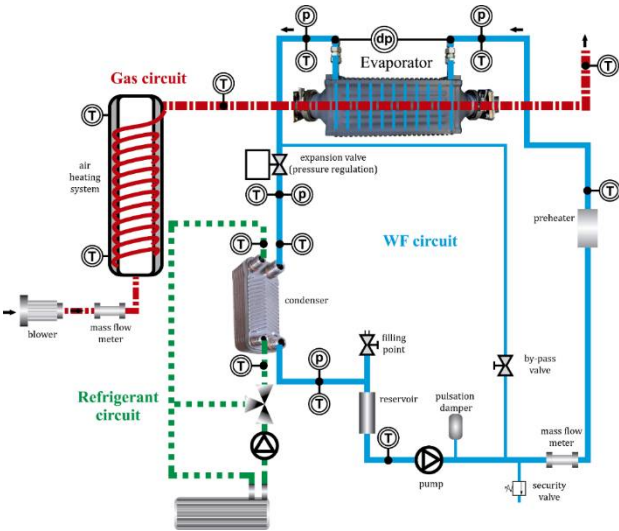
Figure 1. Schematic diagram of the test bench.

The test bench control system is based on a programmable logic controller (PLC). It can be accessed either directly from the test bench or with some complementary software allowing remote access or an SD card suite. Ultimately, the software enables the computer and test bench to exchange information by transferring all the data from the bench to the computer in order to analyse it.

The test bench includes a bypass valve system for safe emptying, cleaning and ethanol dragging, in the event the boiler is replaced to test a different one. The characteristics of the main components of the test bench, with the exception of the boiler itself, which is discussed separately in this section, are listed in Table 1.

Table 1. Main components of the test bench.

	Components	Remarks
Air circuit	Air blower	Power 4W Voltage 345-415 V Maximum flow rate 318 m3/h Maximum pressure drop: 390 mbar
	Air heating	Atmospheric pressure Made of a resistance of 27 kW at 240 V AC Maximum temperature: 750°C
WF circuit	Pump (ethanol)	Power 1.5 kW Maximum flow rate 50 l/h Maximum speed: 233 rpm
	Condenser	Heat exchanger with plates Ethanol refrigerated with water
Water refrigerant	Pump (refrigeration)	Flow rate 3.25 l/h Speed 2820 rpm Power 0.37kW
	Heating unit	Maximum air flow rate 4080 m3/h Refrigeration capacity 20.1 kW Heating capacity: 30.7 kW Maximum water flow rate: 57.6 l/min

Temperature sensors are distributed all along the test bench to provide the air, ethanol and water temperature at different points of the bench. These points include, among others, the evaporator inlet and outlet and the ethanol preheater inlet and outlet, which allow us to characterize these points'

100 thermal efficiencies. Pressure drop sensors are mounted on the working fluid side.   The main sensors
101 of the experimental setup are described in Table 2.

102

Table 2. Description of the main sensors of the test bench.

Sensor	Remarks	Uncertainty
Air	Sensor K	1.5 °C
Water/Ethanol	Sensor T	0.5 °C
Pressure drop	Differential pressure transducer	0.4%
Mass flow rate	Coriolis mass flow meter	0.11%

103
104 The air circuit provides air at a suitable temperature and flow rate to the evaporator after being
105 heated in the heating system. It has three main components: blower, flow rate gauge, and heating
106 system. It basically consists of an open circuit, where air is taken from the environment using an
107 electric turbine as a blower, and a heating system, where the air's temperature is gradually increased
108 until the required temperature before entering the boiler.
109 The ethanol circuit is the operation control most prone to instabilty in the whole system. It is
110 designed to pump the liquid ethanol into the evaporator and then through a condenser, where it is
111 cooled before entering a storage tank being pumped again. The eccentric screw pump pumps the
112 ethanol at the set pressure. Just before entering the boiler, an electric preheater helps the ethanol's
113 temperature to rise to the set temperature. A plate condenser cools the ethanol after the expansion
114 valve. The storage tank stores all the ethanol after it is cooled in the condenser and keeps it at the
115 proper pressure before entering the pump again.
116 The experimental bench also has a refrigeration system that cools the hot ethanol leaving the
117 evaporator and further cools the ethanol before entering the storage tank. The components of this
118 circuit are: a centrifugal pump that   pressurizes the water so it reaches the condenser; a regulation
119 valve, and; a heating unit, which consists of a forced convection air heater. The working fluid for this
120 system is water, which flows through the condenser in counter-current.
121 The boiler studied is a shell and tube heat exchanger in cross flow and counter flow, made
122 entirely of steel AISI 316L. Air flows through a bundle of staggered tubes, while the working fluid
123 flows inside them, in a cross-flow configuration. After the working fluid intake, this flow is divided
124 between the first row of tubes, which at the end converge into a mixture chamber to be divided again
125 in the following row. Every mixing chamber only connects one row of tubes with the following one.
126 The performance of the boiler is monitored continuously with thermocouples measuring inlet and
127 outlet air and working fluid temperatures. Pressure drop on both sides are recorded by pressure
128 sensors and a differential pressure sensor. The boiler has been fully coated in thermal black paint on
129 its external surfaces in order to make a visual contrast with the background and avoid shiny
130 reflections in the surface of metal, which could introduce errors in the measurements with the
131 thermographic camera. This black coating increases the emissivity of thermal radiation of the boiler,
132 which according to the specification of the manufacturer is is equal to 0.98, an effect that is taken into
133 account later in the results discussion. Figure 2 represents the boiler studied and Table 3 summarizes
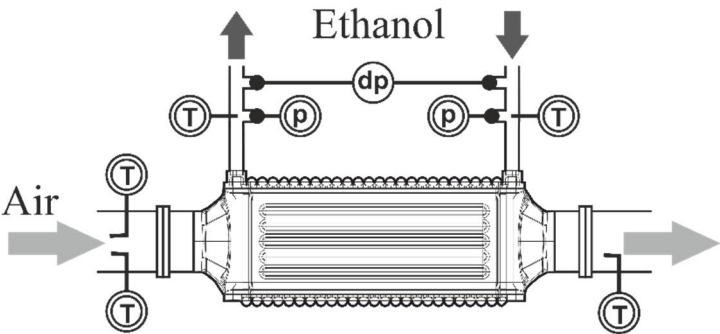134 its geometrical remarks.

135
136

Figure 2. Experimental boiler.

137

138   Wall temperature was monitored using the thermographic camera Flir E60, by Flir Systems.
139 Some technical characteristics of the camera are shown in Table 3.

140   **Table 3.** Main features of the thermographic camera used.

Model	Flir E60
Range of temperature	-20°C to 650°C
Thermal sensitivity	<0.05° to 30°
Resolution	320 x 240 pixels

141 **3. Methodology**

142   The predominant experimental tool used in this study was infrared thermography. The objective
143 of this noninvasive method was to extract a continuous wall temperature profile along the boiler,
144 which provides information about the fluid underneath the walls. This section is divided in two parts:
145 first, the experimental procedure--that is, how the experiments were carried out and what
146 considerations were taken when the thermal images were shot; and second, the post-processing of
147 the thermal images.

148 *3.1. Experimental procedure*

149   The experimental procedure is summarized in Figure 3. To run the experiments at the test bench,
150 the inputs of the circuit are set in the bench software: inlet temperature, pressure, and mass flow rate
151 for both air and ethanol circuits. Firstly, the test bench needs to be warmed up. This is done by
152 gradually introducing the desired values of mass flow and system temperature in the both circuits.
153 It is done to ensure a proper functioning and avoid overheating and any damage to the components.
154 The measurements and the thermal images are taken once the monitored outputs confirm that the
155 test has reached a steady state. Subsequent experiments can be performed using the conditions of the
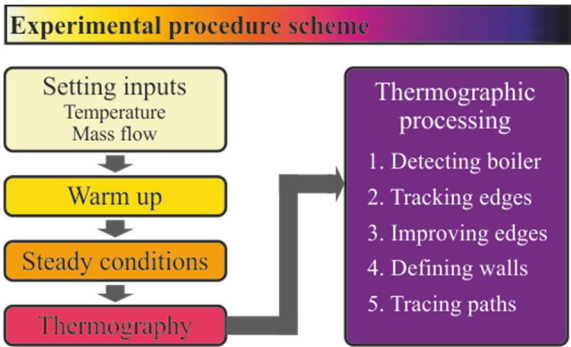156 previous one, without the need to restart the circuit configuration again.

157
158   **Figure 3.** Scheme of the experimental procedure.

159   As shown in Figure 4, from the point of view of the thermal image, the top wall is adjacent to
160 the gas side, whereas the frontal wall is adjacent to the mixing chambers of the working fluid, thus
161 the thermographic analysis of these walls makes it possible to quantitatively learn about
162 thermodynamic behaviour of the fluids inside the boiler. Bearing this idea in mind, the relative
163 positioning of the thermographic camera and the boiler makes it possible to picture two walls at a
164 time, one adjacent to the fluid and the other adjacent to the gas. Figure 4 shows a schematic view of
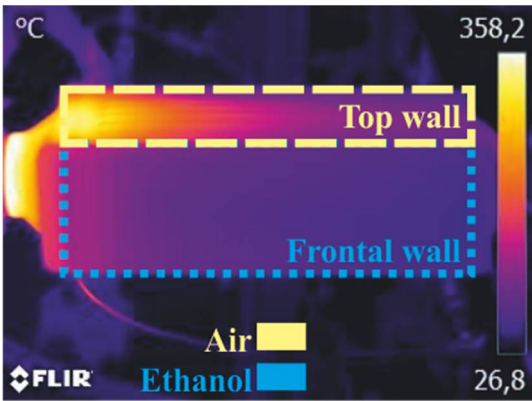165 the perspective of the boiler from the camera.
166

Figure 4. Schematic view of the thermographies.

The images were taken by placing the camera on a tripod at a distance of approximately 50 cm at an angle of about 30° relative to the frontal wall. The thermographic camera used, the model Flir E60, takes pictures with a resolution of 320x240 pixels and can measure in a range of temperatures from 0°C to 650°C with an accuracy of ±2°C or ±2% at room temperature and a sensitivity of 0.05°C.

3.2. Thermographic processing

Raw thermal images were post-processed with the free software Flir Tools. This software can convert the temperature of every pixel into an array of the dimension of the resolution of the camera with the values of temperature in each element. This array is then exported to Matlab in a *.csv file, which performs the calculations needed in this study. The thermal image shows the wall temperature of the boiler, but also the temperatures of the background of the scene. Since these values are not of interest, they were eliminated in the processing.

To do this, a very simple method was tested first. The images were given a temperature limit, and all the pixels (in .csv, a cell and in Matlab, an element of the array) that did not reach a minimum temperature had their values converted to NaN. Then, pixels were arranged by rows and by columns, with all rows and columns with an average value of NaN lower than a certain value being eliminated. To eliminate the hot tubes that do not completely disappear after the previous filtrations, a filtering process was carried out by columns and rows with a minimum number of non-NaN. This method was quite effective, but in cases where the boiler is inclined, the cutting section was too horizontal and some data were lost. Another problem is that the perspective was lost, and thus the construction of the lines in their correct position.

With this in mind, a new methodology was developed. This methodology detects the boiler through a pattern recognition approach. Wall temperature paths were traced and plotted automatically. Wall temperature values in both gas and working fluid regions, both parallel and perpendicular to the flow of the fluids, were tracked. The whole process can be divided in five steps: detecting the boiler, tracking the edges, improving the edges, tracing the walls, and defining the paths. Figure 4 to Figure 9 included in this section are used to illustrate the methodology, and do not represent any particular experimental point.

3.2.1. Detecting the boiler

To identify the shape of the boiler, a temperature difference filter was applied, thus taking advantage of the sharp difference between the boiler's and room temperatures. Some pipes and ducts from the circuit can be seen in the thermal image, but they all belong to the ethanol circuit, whose temperatures are significantly lower than the temperature of the boiler. To filter these out, the first step was to coarsely discard the pixels belonging to the background. To do so, the pixels of temperature below a threshold of 40°C is replaced by black pixels, resulting in an image similar to the displayed in Figure 5-a. Notice that some components of the circuit with higher temperatures than the threshold temperature are still displayed.

205   To discard the remaining undesired pixels, the rows and columns of pixels with less than a
206 threshold number of blank pixels are filtered and set as blank pixels too. A sample of a resulting
207 image is displayed in Figure 5-b. Note that to apply the method shown here, the boiler was positioned
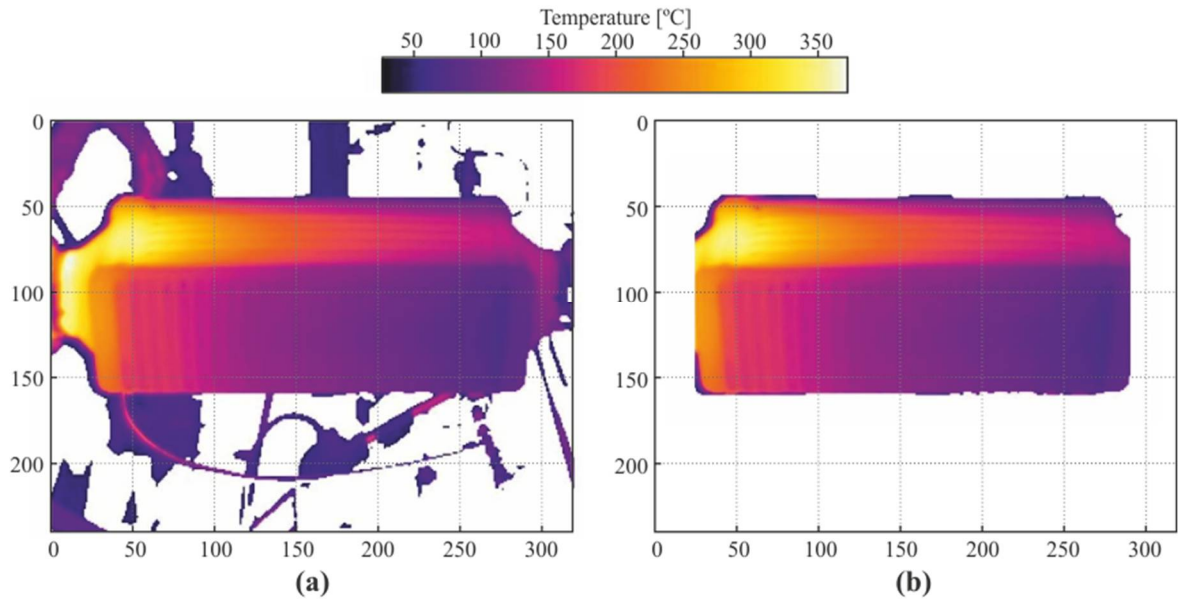208 as horizontally as possible from the perspective of the thermographic camera.

209
210   **Figure 5.** (**a**) Sample of the core of the boiler detected. (**b**) Sample of thermography after filtering cold pixels
211   in the background.

212 3.2.2. Tracking the edges

213   As shown in Figure 5-b, the boundaries of the boiler are still not neatly defined. To identify the
214 horizontal edges of the boiler, the highest wall temperature gradient is chosen as the next filter criterion.
215 In Figure 6, a 3D graph of temperatures of the boiler is plotted. Here, it is clear that the maximum
216 temperature gradient corresponds to the outermost edges of the boiler from the perspective of the
217 camera. The edge between the top wall and the frontal wall becomes an inflection point of the
218 temperature profiles. Figure 7 shows the reconstruction of the edges of the boiler using this approach.
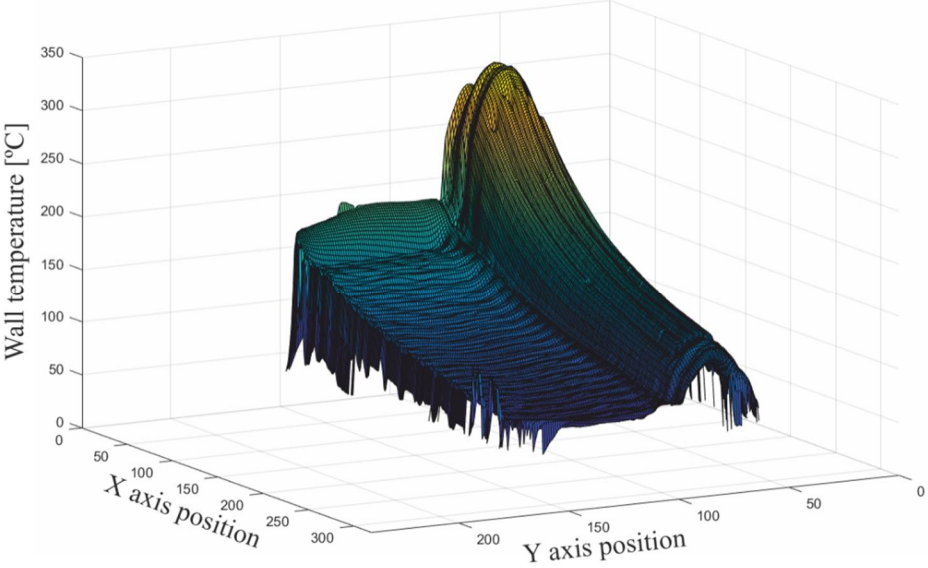

219
220   **Figure 6.** 3D graph of the temperatures identified as belonging to the boiler at this step of the procedure.

221

222   3.2.3. Improving the edges

223   As shown in Figure 7-a, the pixel cloud representing the horizontal edges obtained in the previous
224   step still shows noise and does not seem to be the straight line we know it ought to be. To convert that
225   point cloud into a straight line, two further steps were taken: filtering outliers and a Hough transform
226   [18–20].
227   The outliers were filtered by their deviation from the median of the vertical location of the pixels,
228   when the pixel is an outlier q with the criterion:

$$q < Q_1 - 1.5\,IQR$$

or   (1)

$$q > Q_3 + 1.5\,IQR$$

229   where Q_1 and Q_3 are the first and the third quartile respectively and IQR is the interquartile range.
230   Once the outliers were filtered, Figure 7-b, a Hough transform was applied. A Hough transform is
231   a digital image processing technique based on feature recognition. The technique consists of identifying
232   any geometrical instance that can be parametrized, such as straight lines, circumferences or ellipses.
233   This very effectively converted the remaining point clouds representing the edges into a straight line.
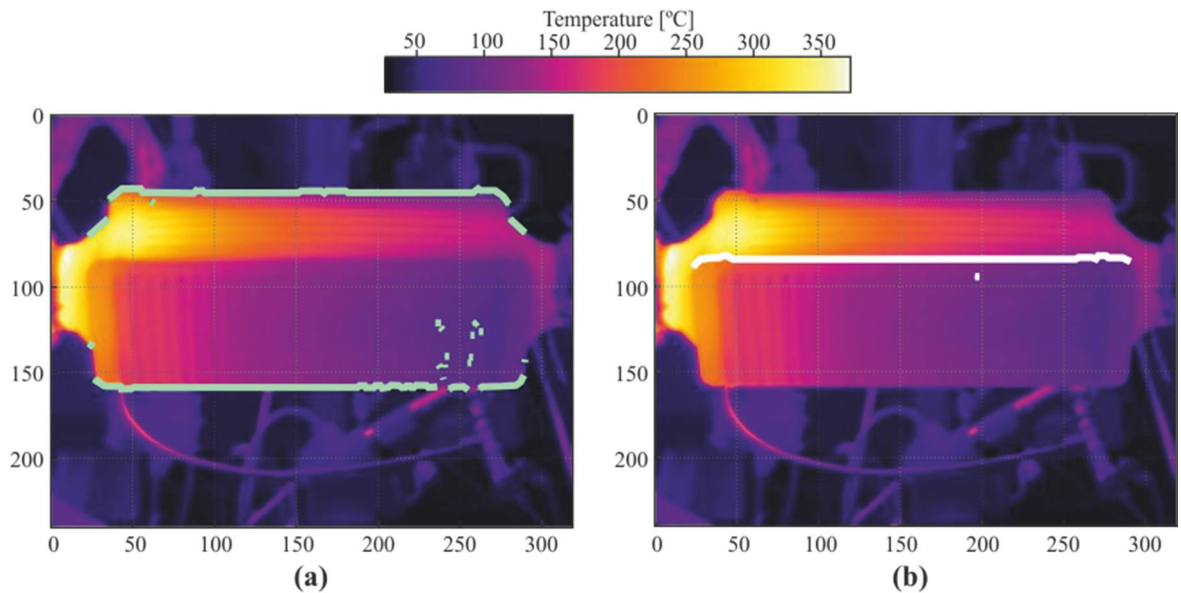

234
235   **Figure 7.** (**a**) The reconstruction of the outermost edges is represented in the colour green. (**b**) The
236   reconstruction of the middle edge is represented in the colour white.

237   3.2.4. Defining the walls

238   Because the output of the Hough transform is a line —and not a geometrical segment— to define
239   the frontal and top walls in the images, the vertices of the now-clear edges must be found.
240   There are two issues to solve in this phase. The first is that although the outliers points should have
241   been filtered by the criterion previously discussed, it was observed that some of these points remained
242   because they belonged to the gas boxes. The second issue is found in the particular boiler used in this
243   study. Due to its manufacturing procedure, the plaque that makes up the superior wall is framed into
244   the gas boxes, deforming it slightly.
245   Taking these two considerations into account, the vertices of the edges are determined by finding
246   the first point at more than two pixels' distances from the line previously found with the Hough
247   transform.
248   Once the horizontal edges on the top and frontal walls are defined (Figure 8-a) the remaining
249   vertical edges are defined by tracing a straight line between the vertices of the horizontal edges, thus
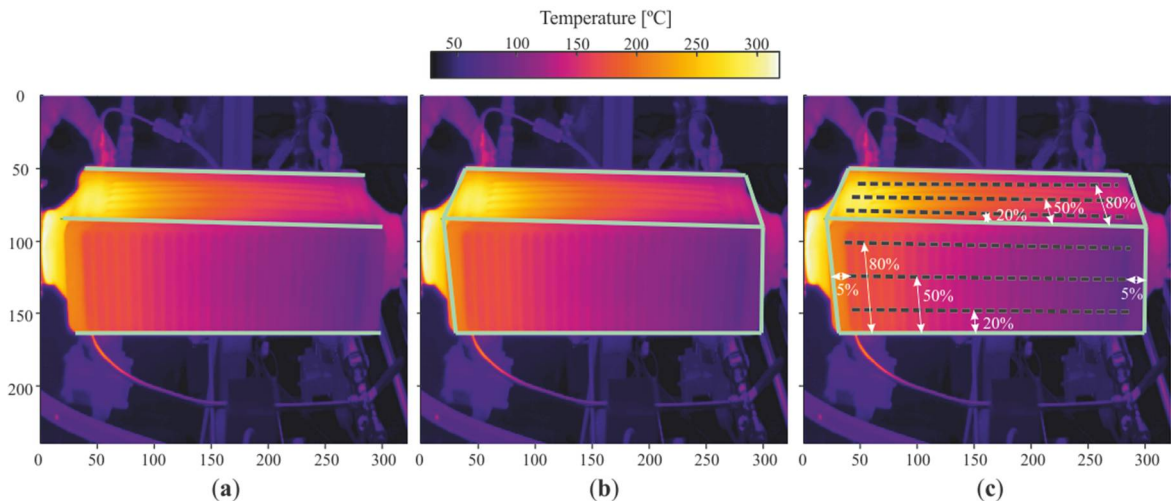250   obtaining the walls of interest, as shown in the graph Figure 8-b.

Figure 8. Walls detected by the developed methodology, (a) main edges detected (b) walls of interest (c) studied paths position.

3.2.5. Tracing paths

Having defined the four edges that define the walls of interest, the path where the properties of wall temperatures is tracked can be defined. Paths of wall temperature are defined on both the frontal and top walls, longitudinal to the flow of both fluids involved. In terms of percentage of the corresponding edge longitude, every path is at 5% away from the vertical edge, and 20%, 50% and 80% away from the middle edge, as shown on the graph Figure 8-c, and in more detail in Figure 9.
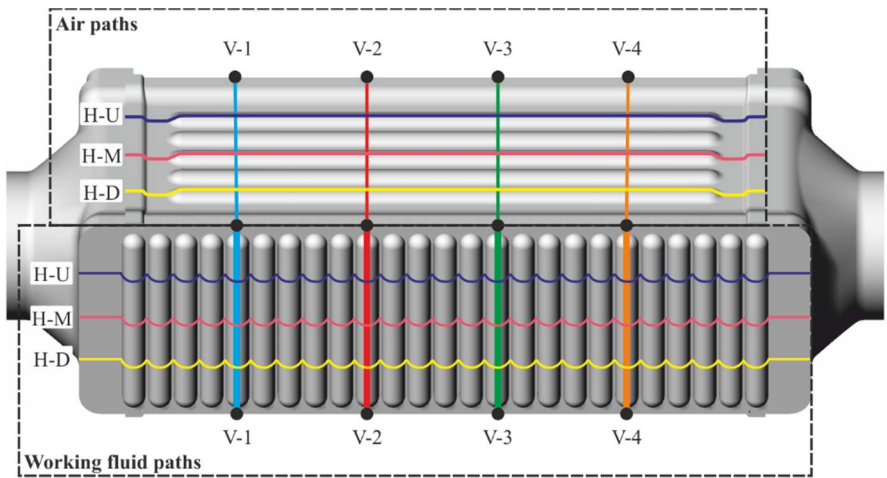

Figure 9. Definition and nomenclature of the paths studied.

To retrieve the value of the temperature of the paths, the paths were divided into 200 points and a two-dimensional interpolation was calculated between the two nearest pixels from the image, with the vertical coordinate as a reference. To reduce the oscillations in the values of wall temperature due to the ripples of the external surfaces in the paths of both the gas and working fluid sides, profiles of the horizontal wall temperature paths were smoothed using the robust local regression method with weighted linear least squares and a second-degree polynomial model, which was carried out using MATLAB software.

4. Results and discussion

Throughout the study, we ran the test under different conditions as a control of the methodology.   The result of the test carried out under the operating conditions, detailed in Table 4, are discuss in this section.
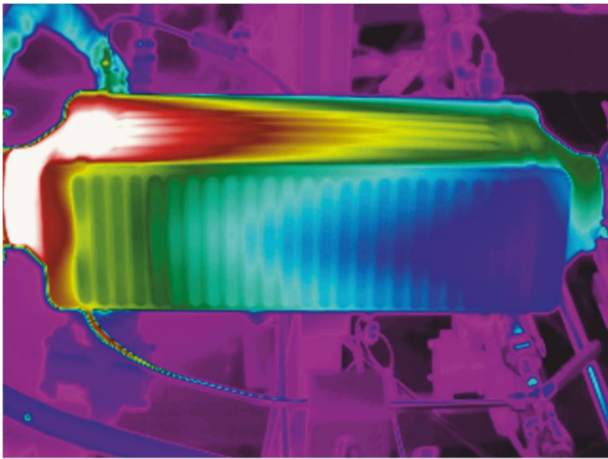
274

Table 4. Boiler operating conditions.

	Ethanol	Dry air
Inlet mass flow [kg/h]	30	70
Inlet temperature [°C]	80	700
Pressure outlet [bar-a]	21	1
Outlet temperature [°C]	275.14	131.44
Performance [%]	85.3	

275
276   Figure 10 shows the thermal image corresponding to the test point previously described.
277

278
279   **Figure 10.** Thermography of the boiler with the operating conditions described in Table 4.

280   The lines in Figure 11-a represent the horizontal profiles of wall temperature in the wall adjacent
281   to the mixture chambers on the working fluid side. The slopes of the curves clearly show 4 stages.
282   From left to right, the first and hotter stage represents the portion of the wall which is adjacent to the
283   gas side. The second stage of the curve shows a portion where there are not great changes in the slope
284   of the curve—in fact it is almost constant—which indicates a phase change on the working fluid side.
285   In the third stage the slope remains negative, indicating that the working fluid is being cooled down
286   in a monophasic flow. In the last stage, wall temperature increases again, where the wall is again
287   adjacent to the gas side.
288   Figure 11-b shows the horizontal paths of wall temperature on the wall adjacent to the gas side,
289   that is, the top wall. As expected, wall temperature decreases along the boiler, while gas is
290   transferring heat to the working fluid and, to a lesser extent, to the environment by free convection
291   and radiation. Figure 12-b shows the vertical paths on the gas side. Notice the wavy pattern of wall
292   temperature, which is easily identified too in a visual analysis of the thermal image in Figure 10.
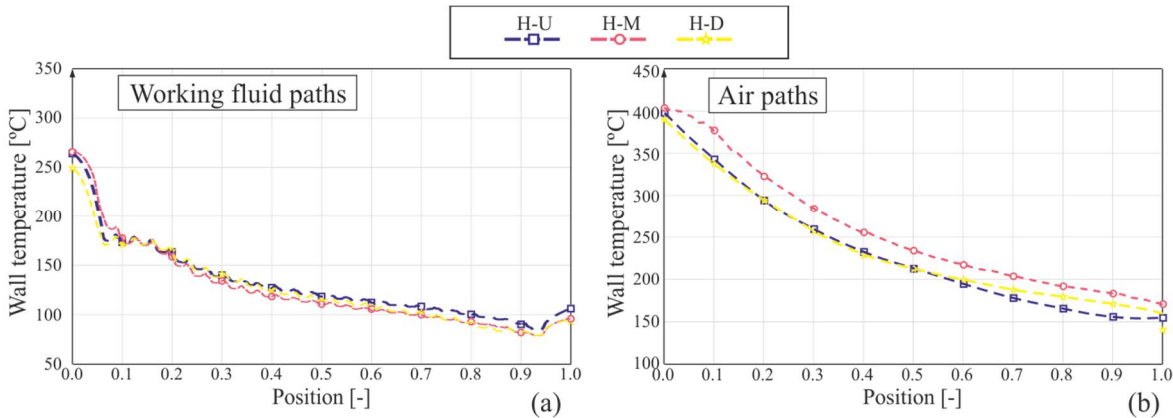
293
294   **Figure 11.** Graphs of horizontal temperature profile: (**a**) WF paths and (**b**) in the air.

295 Although the geometry of the boiler is almost symmetric, wall temperature in the vertical paths
296 of Figure 12-a are not as symmetric as would be expected, being seriously displaced in every case.
297 This is likely to be mainly due to the perspective of the camera with regard to the boiler, which is not
298 orthogonal. The position of the camera was a compromise solution between having the most
299 information possible in a single image and making the process of taking the images as automated
300 and standardized as possible, with no need to change the camera or boiler position twice in every
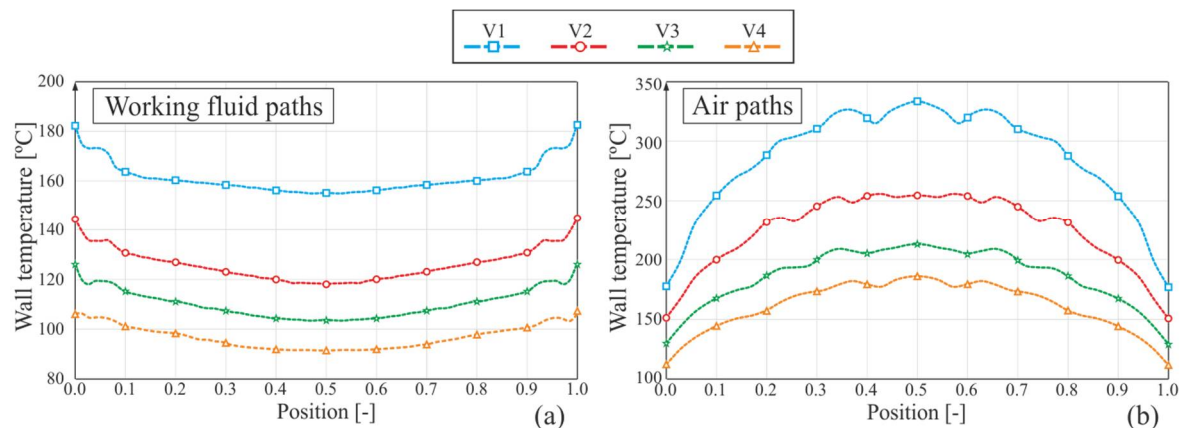301 experiment.

302
303 **Figure 12.** Graphs of vertical temperature profile: (**a**) WF paths and (**b**) in the air.

304 **5. Conclusions**

305 In this study an experimental bench was presented to test boilers for an Organic Rankine Cycle
306 in a waste heat recover system, as well as a methodology to detect and analyse them via pattern
307 recognition with thermography. This methodology is able to handle a large amount of thermal
308 images in a database and automatically extract paths of wall temperatures. These paths could be
309 useful for developing correlations that can be used in predictive —zero-dimensional, one-dimensional
310 or CFD— models.
311 Once the thermal images are analysed, phase transition on the working fluid side is clearly
312 noticeable, identifiable by a stage where wall temperature remains almost constant, in contrast with
313 the remaining length of the path.
314 Future work will focus on the experimental setup, principally by carrying out further analysis
315 of pressure drop in working fluids, and in the thermographic analysis, mainly by comparing the
316 results obtained with a CFD solution and diving deeper into the working fluid phase transition.

319 **Conflicts of Interest:** The authors declare no conflict of interest.

320 **References**

321 1.   Domingues, A.; Santos, H.; Costa, M. Analysis of vehicle exhaust waste heat recovery potential using a
322   Rankine cycle. *Energy.* **2013**, 49, 71–85. https://doi.org/10.1016/j.energy.2012.11.001
323 2.   Park, T.; Teng, H.; Hunter, G.L.; van der Velde, B.; Klaver, J. A Rankine Cycle System for Recovering Waste
324   Heat from HD Diesel Engines - Experimental Results. *SAE International*. **2011**. https://doi.org/10.4271/2011-
325   01-1337
326 3.   Wang, E.H.; Zhang, H.G.; Fan, B.Y.; Ouyang, M.G.; Zhao, Y.; Mu, Q.H. Study of working fluid selection of
327   organic Rankine cycle (ORC) for engine waste heat recovery. *Energy.* **2011**, 36, 3406–3418.
328   https://doi.org/10.1016/j.energy.2011.03.041
329 4.   Wang, T.; Zhang, Y.; Peng, Z.; Shu, G. A review of researches on thermal exhaust heat recovery with
330   Rankine cycle. *Renew. Sust. Energ. Rev.* **2011**, 15, 2862–2871. https://doi.org/10.1016/j.rser.2011.03.015
331 5.   He, M.; Zhang, X.; Zeng, K.; Gao, K. A combined thermodynamic cycle used for waste heat recovery of
332   internal combustion engine. *Energy.* **2011**, 36, 6821–6829. https://doi.org/10.1016/j.energy.2011.10.014

6. Horst, T.A.; Rottengruber, H.S.; Seifert, M.; Ringler, J. Dynamic heat exchanger model for performance prediction and control system design of automotive waste heat recovery systems. *Appl. Energ.* **2013**, 105, 293–303. https://doi.org/10.1016/j.apenergy.2012.12.060

7. Saleh, B.; Koglbauer, G.; Wendland, M.; Fischer, J. Working fluids for low-temperature organic Rankine cycles. *Energy*. **2007**, 32, 1210–1221. https://doi.org/10.1016/j.energy.2006.07.001

8. Schmid, H. Less Emission Through Waste Heat Recovery. In Green Ship Technology Conference, London, U.K., 28-29 April 2004.

9. Teng, H. Waste Heat Recovery Concept to Reduce Fuel Consumption and Heat Rejection from a Diesel Engine. In *SAE International.* **2010**. https://doi.org/10.4271/2010-01-1928

10. Silva, J.J.D; Maribondo, J.F. Analysis of lubricating oils in shear friction tests using infrared thermography. *Infrared Phys. Techn*. **2018**, 89, 291–298. https://doi.org/10.1016/j.infrared.2018.01.023

11. Liu T.L.; Pan, C. Infrared thermography measurement of two-phase boiling flow heat transfer in a microchannel. *Appl. Therm. Eng.* **2016**, 94, 568–578. https://doi.org/10.1016/j.applthermaleng.2015.10.084

12. Hetsroni, G.; Mosyak, A.; Segal, Z.; Ziskind, G. A uniform temperature heat sink for cooling of electronic devices. *Int. J. Heat Mass Transf.* **2002**, 45, 3275–3286. https://doi.org/10.1016/S0017-9310(02)00048-0

13. Xu, J.L.; Zhang, W.; Wang, Q.W.; Su, Q.C. Flow instability and transient flow patterns inside intercrossed silicon microchannel array in a micro-timescale. *Int. J. Multiph. Flow.* **2006**, 32, 568–592. https://doi.org/10.1016/j.ijmultiphaseflow.2006.02.004

14. Li H.; Hrnjak, P. Quantification of liquid refrigerant distribution in parallel flow microchannel heat exchanger using infrared thermography. *Appl. Therm. Eng*. **2015**, 78, 410–418. https://doi.org/10.1016/j.applthermaleng.2015.01.003

15. Leblay, P.; Henry, J.F.; Caron, D. Leducq, D.; Bontemps, A.; Fournaison, L. Infrared Thermography applied to measurement of Heat transfer coefficient of water in a pipe heated by Joule effect. In 11th Quantitative InfraRed Thermography, Naples, Italy, Jun 2012.

16. Carlomagno, G.M.; Cardone, G. Infrared thermography for convective heat transfer measurements. *Exp. Fluids*. **2010**, 49, 1187–1218. https://doi.org/10.1007/s00348-010-0912-2

17. Scaccabarozzi, R.; Tavano, M.; Invernizzi, C.M.; Martelli, E. Comparison of working fluids and cycle optimization for heat recovery ORCs from large internal combustion engines. *Energy*. **2018**, 158. 396–416. https://doi.org/10.1016/j.energy.2018.06.017

18. Duda, R.O.; Hart, P.E. Use of the Hough Transformation to Detect Lines and Curves in Pictures. *Commun. ACM.* **1972**, 15, 11–15. http://doi.acm.org/10.1145/361237.361242

19. Hough, P.V.C. Method for recognizing complex patterns. U.S. Patent 3, 069 654, 1962.

20. Torrente, M.L.; Biasotti, S.; Falcidieno, B. Recognition of feature curves on 3D shapes using an algebraic approach to Hough transforms. *Pattern Recogn.* **2018**, 73, 111–130. https://doi.org/10.1016/j.patcog.2017.08.008